SYNTHESIS OF MULTICOMPONENT ADVANCED COMPOSITE OXIDE NANOMATERIALS – NEW APPROACHES TO OLD INDUSTRIAL METHODS

СИНТЕЗ МНОГОКОМПОНЕНТНЫХ КОМПОЗИТНЫХ ОКСИДНЫХ НАНОМАТЕРИАЛОВ С УЛУЧШЕННЫМИ ХАРАКТЕРИСТИКАМИ – НОВЫЕ ПОДХОДЫ К СТАРЫМ ПРОМЫШЛЕННЫМ МЕТОДАМ

Dr. Danilenko I.[1], Dr Gorban O.[1], M.Sc. Akhkozov L.[1], Prof. Dr. Sci. Konstantinova T.[1]
National Academy of Science of Ukraine, Donetsk Institute for Physics and Engineering NAS of Ukraine, Kiev, Ukraine [1]

igord69@ukr.net, oxanag1@ukr.net, ahkleo@yandex.ru, alta7@ukr.net

Abstract: *A new approach to design of oxide ceramic-ceramic nanocomposites instead of industrial technical ceramics has been proposed. The use of mixing of liquid solutions of reagents instead of powders mixing allows entering in the matrix material the oxide dopants in supersaturated concentrations. The synthesized nanoparticles contain a potential for the formation of various structures. By the controlling of heating regimes during nanopowders sintering processes we can control the diffusion processes on the particles volume and boundaries. The decomposition of initial supersaturated solid solution during heat treatment (especially at fast sintering) can lead to formation of multilevel nanocomposite structure in the ceramic matrix with enhancing mechanical, electrical, optical and magnetic properties. It is established on the example of zirconia that even a slight amount of aluminum oxide, nickel oxide, zinc oxide leads to a significant change of the nanopowders and ceramics properties.*

Keywords: OXIDE NANOPOWDERS, SYNTHESIS METHODS, MICROWAVE, DIFFUSION, SINTERING, APPLICATIONS

1. Introduction

Ceramic materials may be divided on several types concerning their functional properties or application, i.e. refractory or electronics, conventional or advanced, but in all cases the properties of monolithic ceramic materials strongly depend from the starting materials, method of their densification and microstructure of materials [1-3]. Improving of properties of conventional types of ceramic materials to the advanced level may be due to modification of microstructure of traditional ceramic materials. It may be done by several methods, which should balance between expenses and level of properties, because for mass production the level of expenses is a critical parameter too.

Critical factors in the commercialization of advanced ceramics are the starting powders and the method of their densification or sintering. Defects in ceramic materials, such as pores or secondary inclusions, are often introduced by the starting powder, and during forming and densification processes. The cheap coarse starting powders and, consequently, high firing temperature often decrease the level of functional properties of materials, e.g. mechanical strength, density, magnetization, etc. In case of composite materials the amount of critical factors increased in several times, because creation of uniform microstructure of multicomponent composite materials by traditional mixing process is very hard. Now, however, this method is most commonly used in the industry. So, we think, there is one way for improving the properties of composite ceramic materials at the present time. This is the use of mixing of liquid solutions of reagents instead of powders mixing. This is, so called, wet chemical methods, for example precipitation technique [4, 5]. A precipitation reaction is a chemical reaction where one of the products is a precipitate. The use of mixing of liquid solutions of reagents instead of powders mixing allows entering in the matrix material the oxide dopants in supersaturated concentrations. The decomposition of initial supersaturated solid solution during heat treatment (especially fast heating regimes) can lead to formation of multilevel nanocomposite structure in the ceramic matrix with enhancing mechanical, electrical, optical and magnetic properties.

In this study we analyze the structures and functional properties of different types of composite materials obtained by precipitation technique and compare these results with structure and properties of materials, obtained by traditional technology. Also we show that the traditional ceramic technology processes to impose greater restrictions on the chemical composition of materials and parameters of technological process. The materials were used in this study are zirconia based composites with addition of Al^{3+} and Zn^{2+} ions and $LaSrMnO_3$ perovskite.

The both types of materials – zirconia and $LaSrMnO_3$ are well known materials [1-7, 12, 13], which have unique properties and influence of particle size on its properties ("size effect") are easy be demonstrated.

2. Experimental

2.1. Material preparation

ZrO_2-3 mol% ZnO, ZrO_2-3mol% Y_2O_3 (3Y-TZP) and ZrO_2-3mol% Y_2O_3 +n%Al_2O_3 nanopowders were synthesized with a co-precipitation technique using $ZrOCl_2 \cdot nH_2O$, $Y(NO_3)_3 \cdot nH_2O$, $AlCl_3 \cdot 6H_2O$ and $ZnCl_2$ salts. The amount of alumina was varied from 0.5 to 5 wt%. The amount of ZnO was varied from 3 to 50 wt%. All used chemicals were of chemical purity. The technological aspects of the precipitation process were described in [6, 7]. After washing and filtration, the hydrogel was dried in a microwave furnace with an output power of 700 W and at a frequency of 2.45 GHz. The dried zirconium hydroxides and composites were calcined in a resistive furnace at different temperatures with a dwelling time of 2 h. In order to compare our results obtained on ZrO_2-3mol% Y_2O_3 +n%Al_2O_3 with data obtained with Tosoh powders with similar initial zirconia particle sizes the calcination was done at 1000°C.

For the control samples, an appropriate amount of α-Al_2O_3 powder was mixed with obtained 3Y-TZP nanopowders in distilled water. The α-Al_2O_3 particle size distribution was wide enough with an average size at 1 μm (manufacturer's data). In case of ZrO_2 – ZnO composites the different amount of ZnO was mixed with obtained ZrO_2 nanopowders in distilled water. These mixtures were planetary-milled (MSK-SFM-1 MTI Corp., USA) at 400 rpm for 10 h using YSZ milling media. This variant was named BM and this abbreviation marked in powder name.

For synthesis of $La_{0.7}Sr_{0.3}MnO_3$ (LSM) powders we also used the co-precipitation method. Stoichiometric amounts of La_2O_3, $SrCl_2 \cdot 2H_2O$, and $Mn(NO_3)_3 \cdot 6H_2O$ were used as starting materials, and NaOH and Na_2CO_3 were used as precipitants. The LSM nanopowder obtained by precipitation in Na_2CO_3 was labeled as NP1, while the LSM nanopowder obtained by precipitation in NaOH was labeled as NP2. The drying procedure was analogical with previous reported. The firing regimes for the LSM powders were chosen by the formation of the 100% perovskite phase. These temperatures were 850 and 620°C for NP1 and NP2 powders respectively.

2.2. Materials characterization

The powders and sintered specimens were characterized by means of XRD (Dron-3) with Cu-Kα radiation for crystallite sizes

and quantitative phase analyses with a proven method [8]. Particle sizes of different calcined powders were estimated by means of transmission electron microscopy (JEM 200, Jeol, Japan).The optical properties of ZrO_2-ZnO nanopowders were measured on Cary 5000 UV-Vis-NIR spectrometer (Agilent Technologies, USA).

3. Results and discussion

3.1. ZrO_2 - ZnO systems. Powders characteristics and optical properties.

It was found that the structure and optical properties of powders depend from method of powder synthesis and calcining temperature. The light absorption spectra of ZnO, ZrO_2 and their mixes are well known. The absorption peak near 3.2 eV is corresponded to ZnO and absorption level increased with increasing of ZnO concentration for all particle sizes [10]. With increasing of calcining temperature and consequently with increasing ZnO particle size, the ZnO absorption decreased (Fig. 1a). XRD fixed the ZrO_2 and ZnO phases (Fig. 2c). The typical TEM image of ZrO_2 - ZnO particles depicted on Fig. 2.

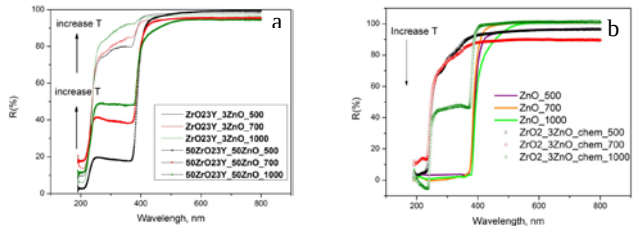

***Fig. 1** The adsorption spectra of ZrO_2-ZnO nanopowders, obtained by mixing technique - a) and coprecipitation – b) and calcined at different temperatures: 500 (black), 700 (red) and 1000°C (green).*

When the ZrO_2-ZnO powder synthesized by coprecipitation technique the absorption near 3.2 eV, which correspond to ZnO adsorption, did not fixed and XRD analysis did not found peaks which correspond to ZnO after calcination at temperatures less 700°C. After calcinations at 1000°C the absorption peak appeared and ZnO was fixed by XRD (Fig.2d). But the absorption level in this case in tens times higher in comparison with powders obtained by mixing technique. As you can see the absorption level of 50% ZnO in mixed sample equivalent of 3% ZnO in sample obtained by precipitation. So, distribution ZnO in ZrO_2 in this case is differing in comparison with powders obtained by mixing technique (Fig. 2).

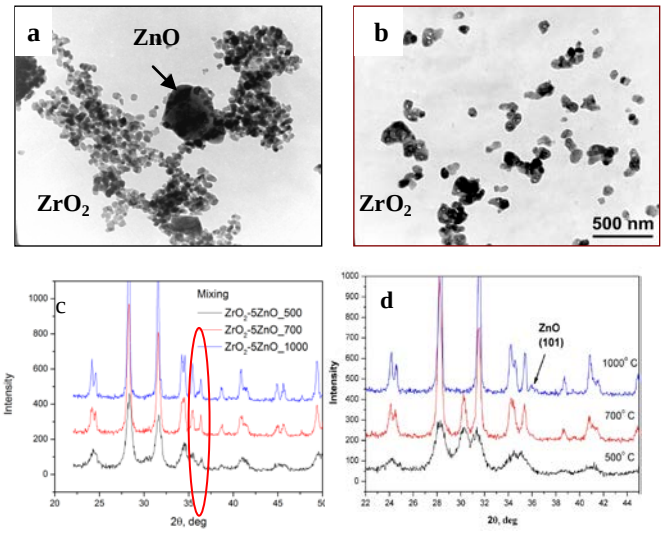

***Fig.2** TEM images of ZrO_2-ZnO nanopowders, obtained by mixing - a) and coprecipitation – b) techniques and calcined at 700°C. The XRD spectra for ZrO_2-ZnO obtained by mixing –c) and coprecipitation – d).*

From previous works of Stefanic it is known that ZnO is not stabilized the ZrO_2 lattice [11], and, consequently, did not form the solid solution in ZrO_2 lattice. But when we use the coprecipitation technique we can create conditions (at low firing temperatures) when the nonequilibrum solid solutions are exist. We think when Zn atoms are located in nonequilibrum solid solution in ZrO_2 lattice the absorption spectrum was determined by ZrO_2, when ZnO diffused from ZrO_2 particles the absorption which correspond ZnO is appear. For data comparation the adsorption spectra of pure ZnO, calcined at different temperatures were also shown on figure 1b.

3.2. LSM nanopowders and their magnetic properties.

In our study [12], we showed that the magnetization of LSM nanopowder (NP2) with average particle size 20 nm is three times less than LSM nanopowder (NP1) with wide particle size distribution (Fig. 3).

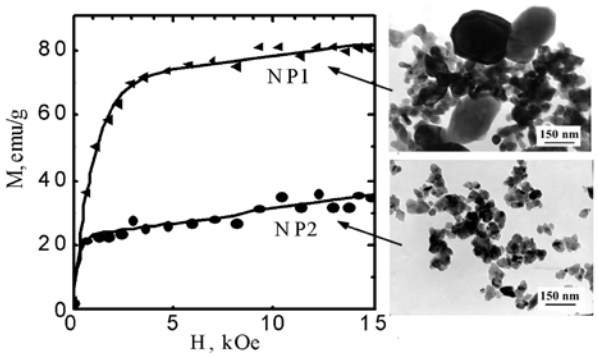

***Fig. 3** Magnetization curves for bimodal (30 nm and 200 nm) (NP1), and 20 nm (NP2) $La_{0.7}Sr_{0.3}MnO_3$ powders at T = 77 K. From [12].*

It was shown that this drastic decrease in magnetization is due to the formation of a magnetically dead layer at the surface, the thickness of which can even increase as the particle size decreases [12, 13]. Also, as was shown previously, a drastic difference in the spin-echo signal intensities for NP1 and NP2 samples was shown, which does not correlate with the decrease in value of the saturation magnetization. This was attributed to the fact that 20 nm nanoparticles are single magnetic domain particles, while the particles of 50 nm and larger in size possessed a multi-domain magnetic structure. The measuring of spin-echo signal intensity of the NP1 and NP2 samples under identical conditions showed that the curve's form of the NP1 sample is typical for multidomain ferromagnetism (an asymmetric curve with one peak), while the curve for the NP2 sample was oscillating and damped. It was concluded that the NP2 nanoparticles were mono-domains in comparison with typical poly-domain NP1 particles. These changes in the magnetic properties of LSM nanopowders were associated with changes in the structure of the powder, which in turn were related to differences in the method of obtaining the powders.

In case of the NP1 powder, the decomposition of CO_3 precursors was used as a method of powder obtaining method. This method is quite close to simple industrial methods of different powders preparation by decomposition of salts and raw materials. Changing the precipitation agent to NaOH led to the formation of an amorphous structure of sediments instead of a crystalline(Fig. 4).

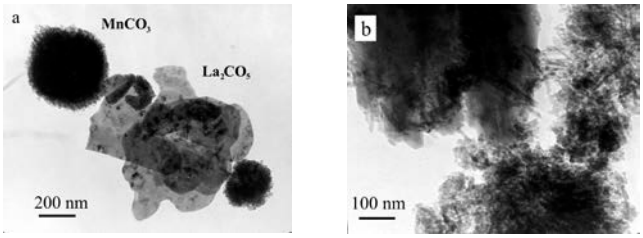

***Fig. 4** TEM images of lanthanum and manganese carbonate - a) and lanthanum and manganese hydroxides –b) – precursors of different methods of LSM powder synthesis processes.*

The formation of two generations of crystals of precursor materials (plate-like lanthanum carbonate and needle-like manganese carbonate) (Fig. 4a) led to the formation of LSM nanoparticles with wide particle size distribution. Besides, the

carbonated salts are needed the high temperature of decomposition and the formation of 100% of LSM perovskite phase finalized only at 850-900°C. This high temperature level is promoted the nanoparticles agglomeration and multi-domain magnetic structure formation.

Changing the precipitation agent to NaOH led to the formation of the amorphous structures of lanthanum and manganese hydroxides (Fig. 4b). Heating of these sediments did not lead to the formation of complex multidimentional structures in comparison to the previous case because the precursors had a homogenous amorphous structure and low temperature of decomposition. The formation of oxide particles in NP2 passed at 600 – 620°C with the formation of small (20–30 nm) particles (Fig. 3). The absence of large LSM particles in the NP2 powder led to the formation only single-domain magnetic particles. These structure changes lead to drastically changing the magnetic properties of LSM powders from ferromagnetic to superparamagnetic.

3.3. Zirconia-alumina composites. Structure and properties.

TEM results of zirconia and zirconia-alumina composite powders are shown in Fig. 5. According to the TEM and XRD data, the average particle size of matrix 3Y-TZP nanopowder was 32 nm (Fig. 5a). Zirconia in the powders was represented by the tetragonal phase (space group P42/nmc) (Fig.6).

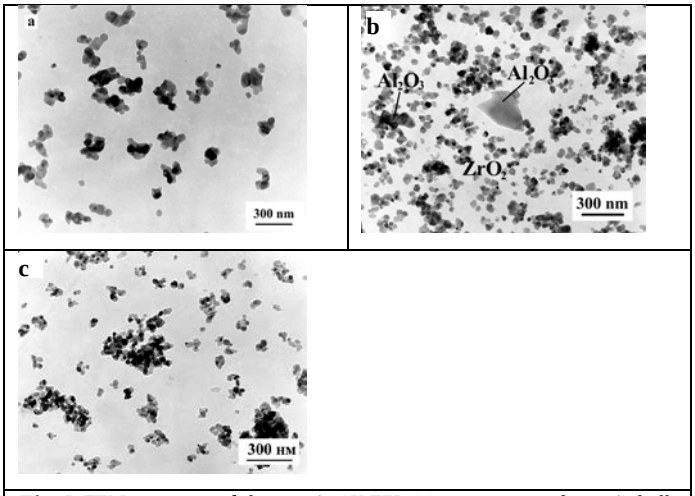

Fig. 5 *TEM structure of the matrix 3Y-TZP 32 nm nanopowder - a), ball-milling 32 nm 3Y-TZP powder with 2w% a-Al_2O_3 – b) and 3Y-TZP-2w% Al_2O_3 obtained by the co-precipitation technique – c).*

The composite powder obtained by ball-milling 32 nm 3Y-TZP nanopowder with commercial α-Al_2O_3 powder is shown in Fig. 5b. After milling, the particle sizes of ZrO_2 did not change. The TEM investigation could not distinguish zirconia and crushed alumina particles smaller than 40 nm, so particles larger than 40 nm were α-Al_2O_3. The average particle size of α-Al_2O_3 particles after milling process was estimated at 150 – 200 nm. From XRD data (peak on 43,36°) we can identify the α-Al_2O_3 in the composite powder that was obtained with the ball-milling technique (Fig. 6b).

According TEM and XRD data the mean particle size of nanopowders obtained with the co-precipitation technique decreased from 32 to 19.3 nm with increasing concentrations of Al_2O_3 from 0 to 5 wt%, respectively. In contrast with previous data, in the nanocomposite powder obtained with the co-precipitation technique, the (101) α-Al_2O_3 reflex was not found during powder characterization (Fig. 6c). The XRD investigation also determined that the lattice parameters (***a***, ***c***) and lattice volume (***V***) of T-ZrO_2 changed from a = 0.50934nm, c = 0.51682 nm, V = 0.13408 nm^3 for matrix 3Y-TZP powder to a = 0.509162 nm, c = 0.516377 nm, V = 0.13386 nm^3, for 3Y-TZP-2wt% Al_2O_3, obtained by co-precipitation technique. In case of 3Y-TZP-2wt% Al_2O_3, obtained by ball-milling technique such changes did not found.

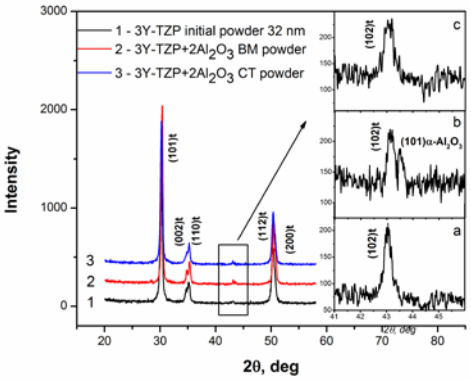

Fig. 6 *XRD data of 3Y-TZP and 3Y-TZP-2wt% Al_2O_3 powders. Initial 3Y-TZP – 1, a), 3Y-TZP-2wt% Al_2O_3 composite obtained with the ball-milling technique – 2, b) and co-precipitation technique – 3, c). In the inserts, the regions 40 – 45° are shown.*

This behavior allows us to decide that Al^{3+} ions formed the solid solution in zirconia lattice. We think that the incorporation of Al^{3+} cations into the ZrO_2 particles limited its crystallization and consequently decreased the particle size of zirconia-alumina composite powders during calcination. The analogical behavior we observed earlier in ZrO_2-Y_2O_3-Cr_2O_3 system [14]. According to XRD results, the phase composition of zirconia after sintering in composites and matrix materials was identical. The phase composition was 9 – 11 % cubic phase and the rest tetragonal phase with equal lattice parameters. Alumina in the all sintered composites was represented by α-Al_2O_3. So, during high temperature treatment the phase compositions are leveling. In our opinion such differences were the main reason for significant changes in the structure and properties of ceramic composites, synthesized by different methods.

Calculation the fracture toughness values shows that the K1C values of CT composites increased more than 40% in comparison with traditional mixing technique (K1C = 5.8±0.4 MPa*$m^{1/2}$) for all Al_2O_3 concentrations, which were studied in this work. The maximal values of K1C (11.2±0.6 MPa*$m^{1/2}$) were found at Al_2O_3 concentrations 1-2 w%. In case of composites obtained by BM technique the monotonic increasing K1C values did not exceed 10% (maximal value 6.7 MPa*$m^{1/2}$ at 5wt%Al_2O_3). The detailed observation of full data can be found in our previous study [15]. The higher value of fracture toughness of the CT composite is explained by the increase in number of crack deviations as well as crack deflection angles. It is also observed by means of SEM that in the CT and BM composites, the part of transcrystalline fracture (Fig. 7 b,c) is higher than that in the matrix material (Fig. 7a), where the intercrystalline fracture mode was predominant.

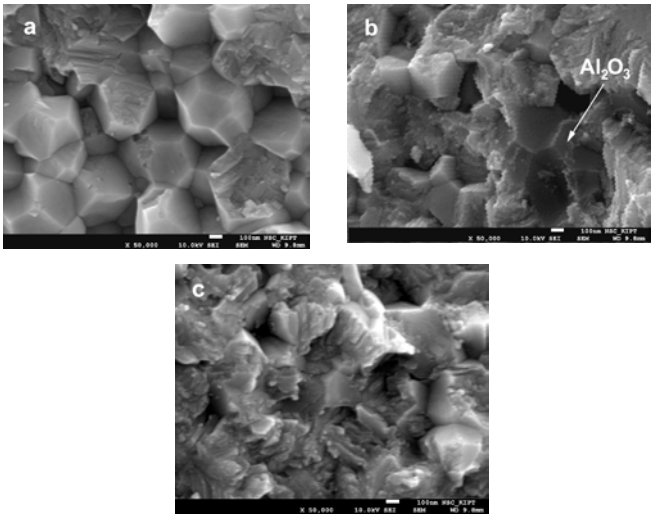

Fig. 7 *SEM images show the increase in the part of transcrystalline fracture in 3Y-TZP- Al_2O_3 composites – b, c) in comparison with matrix 3Y-TZP material – a). Structure of BM composite – b) and CT composite – c).*

When the method of co-precipitation is used, Al^{3+} ion are located in zirconia lattice. Al^{3+} solubility in zirconia is very low, and during sintering the active diffusion of ions Al^{3+} from the volume to the grain boundary or triple junctions takes place. The process of grain growth during sintering of co-precipitated nanopowders is competing with Al^{3+} segregation. Some inclusions can be captured by growing grains and turn into intratype inclusions [16]. An amount of alumina can remain on sub-grains and grains boundaries. The final structure consists of matrix grains and sub-grains with or without alumina segregations, inter- and intratypes of inclusions. The crack propagation from such a structure should be hampered.

Because the mixing process basically is inhomogeneous procedure, the small amount of Al_2O_3 particles can not be uniform distributed in zirconia matrix. In the case of ball-milling powder preparation method, the initial Al_2O_3 particles located only on zirconia grain surfaces and all structure changes took place near the it starting location, so intragranular alumina inclusions in zirconia grains during sintering could not be formed in appropriate amount as well as Al^{3+} segregations, because the mobility and solubility of Al^{3+} ions in zirconia is too low.

Thus, the increase in the K1C value of zirconia ceramics with a small amount of alumina sintered from nanopowders obtained using co-precipitation techniques can be conditioned through a series of processes for composite structure formation during precipitation, crystallization, and sintering of nanopowders. These processes differ strongly from structure formation processes in composites produced from ball-milled powders.

The monolithic ceramic articles obtained from CT synthesized ZrO_2-Al_2O_3 nanopowders with small amount of alumina (1-2 w%) demonstrate the increasing the wear resistance on 40% in comparison with matrix zirconia material [17]. This material can be successfully use for increasing life time of valves, nozzles and other ceramic details as well as for dentistry and bone restoration (Fig. 8). Such small changes in the manufacturing process of the powders production can be easily made within the enterprises.

Fig. 8 *Examples of ceramic articles*

Conclusion

In this study on many examples were shown that industrial powder and ceramic technologies can be improving by including in technology process small amount of dopants in soluble state.

This technology approaches lead to creation of nonequilibrum supersaturated solid solutions, which are partially or fully destroyed during calcination process. The process of dopant migration from grain volume to the grain surface lead to creation of complex multilevel composite structures such as ion segregation on zirconia grain boundaries, clusters, intra- and intercrystalline inclusions in zirconia grains. These processes differ strongly from structure formation processes in composites produced from industrial ball-milled powder.

Acknowledgments

This work was supported by the EU project 691010 – HUNTER and project 47/15H program NAS of Ukraine "Fundamental problems of creation of new nanomaterials and nanotechnologies". We are grateful to NSC KIPT (Kharkov) for SEM analysis.

References

1. Lopez-Esteban S. Mechanical properties and interfaces of zirconia/nickel in micro-and nanocomposites - J. Mater. Sci., 41, [16], 2006, 5194 – 5199. (Lopez-Esteban, S, T. Rodriguez-Suarez, F. Esteban-Betego, C. Pecharroma, J. Moya)
2. Vasylkiv O. Low-temperature processing and mechanical properties of zirconia and Zirconia-Alumina nanoceramics - J. Am. Ceram. Soc., 86, [2], 2003, 299-304. (Vasylkiv, O, Y. Sakka, V. Skorokhod).
3. Naglieri V. Elaboration of alumina-zirconia Composites: role of the zirconia content on the microstructure and mechanical properties - Materials, 6, [5], 2013, 2090-2102. (Naglieri, V, P. Palmero, L. Montanaro, J. Chevalier).
4. Chatterjee M. High Purity Zirconia Powders via Wet Chemical Processing: A Comparative Study - Ceramics hlternational 18, 1992, 337-342. (Chatterjee, M, J. Ray, A. Chatterjee, D. Ganguli).
5. Oliveira A.P. The influence of precipitation variables on zirconia powder synthesis - Powder Technology, 119, 2001, 181–193. (Oliveira A.P., M.L. Torem).
6. Pilipenko N. Peculiarities of zirconium hydroxide microwave drying process - Functional Materials, 9, [3], 2002, 323-327. (Pilipenko, N, T. Konstantinova, V. Tokiy, I. Danilenko, V. Saakjants, V. Primisler).
7. Konstantinova T. Mesoscopic phenomena in oxide nanoparticles systems: processes of growth - J. Nanopart. Res., 13, [9], 2011, 4015-4023. (Konstantinova, T, I. Danilenko, V. Glazunova, G. Volkova, O. Gorban).
8. Garvie R.C. Phase analysis in zirconia systems - J. Am. Ceram. Soc., 55, [6], 1972, 303–305. (Garvie, R.C, P.C. Nicholson).
9. Niihara K. A fracture mechanics analysis of indentation-induced palmqvist crack in ceramics - J. Mater. Sci. Lett., 2, [5], 1983, 221-223.
10. Serpone N. Size Effects on the Photophysical Properties of Colloidal Anatase TiO_2 Particles: Size Quantization or Direct Transitions in This Indirect Semiconductor? - J. Phys. Chem. 99, 1995, 16646-16654. (Serpone, N, D. Lawless, R. Khairutdinov).
11. Štefanic G. Phase development of the ZrO_2–ZnO system during the thermal treatments of amorphous precursors – J. Mol. Struct., 924–926, 2009, 225-234. Štefanic, G, S. Music, M. Ivanda).
12. Danilenko I. $La_{0.7}Sr_{0.3}MnO_3$ nanopowders: Synthesis of different powders structures and real magnetic properties of nanomanganites - Mater. Charact., 82, 2013, 140-145. (Danilenko, I, T. Konstantinova, G. Volkova, V. Glazunova).
13. Krivoruchko V. Magnetic resonances spectroscopy of nano-size particles $La_{0.7}Sr_{0.3}MnO_3$ – JMMM. 300, 2006, 122-125. (Krivoruchko, V, T.Konstantinova, A. Mazur, A. Prokhorov, V. Varyukhin).
14. Konstantinova T. Properties of nanocrystalls tetragonal zirconia in the ZrO2—Y2O3—Cr2O3 system - Nanosystems, Nanomaterials, Nanotechnologies, , 6, [4], 2008, 1147-1158. (Konstantinova, T, V. Tokiy, I. Danilenko, G. Volkova, S. Gorban, N. Tokiy, D. Savina).
15. Danilenko I. The Role of Powder Preparation Method in Enhancing Fracture Toughness of Zirconia Ceramics with Low Alumina Amount – J. Ceram. Sci. Tech., 6, [3], 2015, 191-200. (Danilenko, I, T. Konstantinova, G. Volkova, V. Burkhovetski, V. Glazunova).
16. Matsui K. Phase-transformation and grain-growth kinetics in yttria-stabilized tetragonal zirconia polycrystal doped with a small amount of alumina - J. Eur. Ceram. Soc., 30, [7], 2010, 1679-1690, (Matsui, K, H. Yoshida, Y. Ikuhara).
17. Danilenko I. Effect of small amount of alumina on structure, wear and mechanical properties of 3Y-TZP ceramics – W. J. Eng., 11, [1], 2014, 9-16. (Danilenko, I, S. Prokhorenko, T. Konstantinova, L. Ahkozov, V. Burkhovetski, V. Glazunova).